

## Blue Shift in the Oriented Cuprous Oxide Micro Structures Prepared *via* PEG-400 as the Soft Template by $\gamma$ -Irradiation

WEIJUN LIU\*, ZHICAI HE and GUANGHONG HE

Department of Polymer Science and Engineering, School of Pharmaceutical and Chemical Engineering, Taizhou University, Linhai 317000, Zhejiang Province, P.R. China

\*Corresponding author: Fax: +86 576 85137088; Tel: +86 576 85137182; E-mail: lwj3600@mail.ustc.edu.cn

(Received: 10 September 2010;

Accepted: 11 July 2011)

AJC-10153

Cuprous oxide ( $\text{Cu}_2\text{O}$ ) crystals with platelates structures were synthesized *via*  $\gamma$ -irradiation reducing reaction under ambient conditions, the polyethylene glycol-400 (PEG-400) as non-ionized surfactant and ethylenediamine tetraacetic acid disodium salt ( $\text{Na}_2\text{EDTA}$ ) as chelator of  $\text{Cu}^{2+}$  ions. XRD and FESEM were used to illustrate  $\text{Cu}_2\text{O}$  crystals with platelates structures. The products were also been characterized by HRTEM, ED analysis and UV-VIS absorption spectrum. All the results indicated that the  $\text{Cu}_2\text{O}$  crystals with platelates were successfully prepared under  $\gamma$ -irradiation. The possible mechanism is that the existence of EDTA ions and polyethylene glycol may make growth rate along the  $\langle 111 \rangle$  direction far exceeding that of the  $\langle 100 \rangle$  direction, leading to the formation of platelate structure  $\text{Cu}_2\text{O}$  at last. Its UV-VIS absorption peak revealed blue shift phenomena, with the corresponding band gap of 2.25 eV, the size effect resulted in an obvious blue shift.

**Key Words:** Nanoparticles, Electron microscopy,  $\gamma$ -Irradiation, Optical properties.

### INTRODUCTION

The properties of nanocrystals depend not only on their composition, but also on their structure, phase, shape, size and size distribution. Furthermore, the architectural control of nanosized materials with well-defined shapes is important for the success of "bottom-up" approaches toward future nanodevice<sup>1,2</sup>. And such nanodevices have potential applications in nanoelectronic devices, nanooptical devices and chemical sensors<sup>3,4</sup>, *etc.* To develop ways of tailing the nanomaterials with desired morphologies is quite important and difficult. The ability to manipulate the morphology, size and size distribution of inorganic nanomaterials remains an important goal in modern materials chemistry. The shape of inorganic nanocrystals has much influence on their widely varying physical properties<sup>5,6</sup>. Thus, the synthesis of inorganic nanocrystals of controlled shape arouses great interest. A series of relevant efforts has been paid on the shape' control, the synthesis of single crystalline nanocrystals with advanced structure is still in the developing stage.

Copper oxide ( $\text{Cu}_2\text{O}$ ) nanostructures have attracted significant attention as it is one of the first known *p*-type direct band gap semiconductor with a band gap of 2.17 eV<sup>7,8</sup>. This makes it a promising material for the conversion of solar

energy into electrical or chemical energy<sup>9-11</sup>. The growing interest in  $\text{Cu}_2\text{O}$  nanostructures is due to several reasons. Some of these are (i)  $\text{Cu}_2\text{O}$  is a potential photovoltaic material which is low cost, nontoxic and can be prepared in large quantities<sup>12,13</sup>, (ii) excitons created in  $\text{Cu}_2\text{O}$  have been shown as suitable candidates for Bose Einstein condensate because of the large exciton binding energy of 150 meV<sup>14</sup> and (iii)  $\text{Cu}_2\text{O}$  has been reported to act as a stable catalyst for water splitting under visible light irradiation<sup>15,16</sup>. The  $\text{Cu}_2\text{O}$  nanostructures have been prepared by several methods such as (water-ethylene glycol) mixed-solvothermal route<sup>17</sup>, seed-mediated synthesis<sup>18</sup>, Ultrasonic radiation<sup>19</sup>, *etc.* Based on these approaches, synthesis of  $\text{Cu}_2\text{O}$  nanostructures demands complex process control, high reaction temperatures, long reaction times, expensive chemicals and specific method for specific nanostructures.

In this paper, we developed a facile synthesis of micrometer-sized  $\text{Cu}_2\text{O}$  crystals with platelates structures *via*  $\gamma$ -irradiation and surfactant-assisted under ambient conditions.

We used EDTA as chelator of  $\text{Cu}^{2+}$  ions, PEG-400 (polyethylene glycol-400) as non-ionized surfactant and hydrated electrons generated by  $\gamma$ -radiolysis of water as reductive agents to obtain micrometer-sized  $\text{Cu}_2\text{O}$  crystals with platelate structures *via* nucleation and anisotropic crystal growth processes under room temperature and ambient pressure.

## EXPERIMENTAL

All the reagents purchased from the Shanghai Chemical Company, such as cupric chloride ( $\text{CuCl}_2$ ), ethylenediamine tetraacetic acid disodium salt ( $\text{Na}_2\text{EDTA}$ ), polyethylene glycol-400 (PEG-400), sodium hydroxide ( $\text{NaOH}$ ), isopropyl alcohol and *n*-propyl alcohol, were analytically pure and used without further purification. Distilled water (DI) was used for all solution preparation.

In a typical procedure, 0.31 g of  $\text{CuCl}_2$ , 0.40 g of  $\text{Na}_2\text{EDTA}$  and 2.56 g of PEG-400 (with the concentration of 0.40 mol/L) were dissolved in 16.00 mL of distilled water and 4 mL isopropyl alcohol (as a scavenger of oxidative radicals such as  $\cdot\text{OH}$ ). This solution was stirred for 0.5 h to ensure that the PEG,  $\text{Na}_2\text{EDTA}$  and  $\text{CuCl}_2$  dissolved completely. Then, 4.0 mol/L aqueous  $\text{NaOH}$  solution was added drop-wise to adjust pH = 12-13. Finally, the obtained blue solution was intensively stirred for 1 h at room temperature and then placed in the field of a  $1.30 \times 10^{15}$  Bq  $^{60}\text{Co}$   $\gamma$ -ray source at a dose rate of 38 Gy/min for different time to absorption different absorbed dose (kGy) (sample 1-5). The same recipe for sample 6 was in the absence of PEG-400 (absorbed dose 57.00 kGy). After irradiation, the brick red precipitates were collected and washed with acetone and distilled water for three times, respectively, then dried in a vacuum oven for 24 h at 5 °C. The experimental conditions were summarized in Table-1.

TABLE-1  
IRRADIATION-TEMPLATE METHOD TO FABRICATE  
ORIENTED CUPROUS OXIDE PLATELETS\*

Sample	PEG (g)	Time (h)	Absorbed dose (kGy)	Shape	Size ( $\mu\text{m}$ )
1	2.56	5	11.40	Irregular	0.2-0.5
2	2.56	10	22.80	Platelates	0.4-0.7
3	2.56	15	34.20	Platelates	0.4-1
4	2.56	20	45.60	Platelates	0.5-1.5
5	2.56	25	57.00	Platelates	0.5-1.5
6	–	25	57.00	Nanocluster	0.4

\*The polymerizations were carried out in  $\text{CuCl}_2$  (0.31 g),  $\text{Na}_2\text{EDTA}$  (0.40 g), PEG-400 (2.56 g) distilled water (16 mL) and 4 mL isopropyl alcohol at a dose rate of 38 Gy/min for different time to absorption different absorbed dose.

The powder X-ray diffraction pattern of as-synthesized samples was recorded with a Japan Rigaku D/max  $\lambda_{\text{A}}$  X-ray diffractometer equipped with graphite monochromatized  $\text{CuK}_{\alpha}$  irradiation ( $\lambda = 0.154178$  nm). The scan rate of  $0.06^\circ \text{ s}^{-1}$  allowed to record the pattern in the  $2\theta$  range of  $20$ - $80^\circ$ . The selected area electron diffraction (SAED) patterns were recorded on a JEOL-2010 TEM at an acceleration voltage of 200 kV. FESEM (JEOL JSM-6700) with the acceleration voltage of 5 kV Ultraviolet-visible (UV-VIS) absorption spectrum was recorded by dispersing  $\text{Cu}_2\text{O}$  platelates in distilled water on a UV-2100 Shimadzu spectrophotometer at room temperature.

## RESULTS AND DISCUSSION

Fig. 1. shows the XRD patterns of sample 2 and 4. All of the reflection peaks can be indexed to platelets  $\text{Cu}_2\text{O}$  (JCPDS No. 05-0667). No other diffraction peaks arising from possible impurities such as Cu and  $\text{CuO}$  were detected, indicating

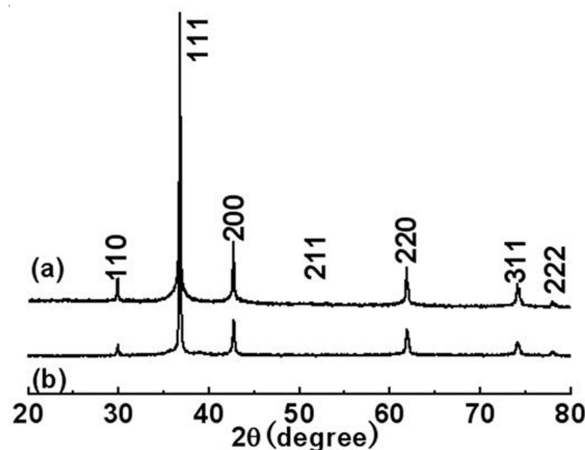


Fig. 1. XRD patterns of (a) sample 2; (b) sample 4

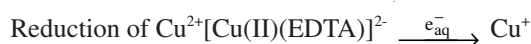
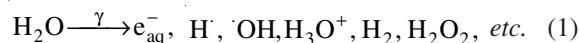
pure  $\text{Cu}_2\text{O}$  was obtained under this experimental condition. The high intensity of the  $\{111\}$  diffraction peak is probably due to the orientation of the crystals suggesting that the obtained crystals are mainly dominated by  $\{111\}$  facets and the  $\{111\}$  planes tend to be preferentially oriented parallel to the surface of the supporting substrate.

The reaction reagents and shape of  $\text{Cu}_2\text{O}$  crystals with platelate structure are summarized in Table-1. The shape and size of  $\text{Cu}_2\text{O}$  crystals with platelates structure were characterized by FESEM as shown in Fig. 2. Fig. 2. give the different shape of  $\text{Cu}_2\text{O}$  crystals according to the different absorbed dose at a dose rate of 38 Gy/min. When the absorbed dose is 11.40 KGy, the FESEM is shown in Fig. 2a. When make the absorbed dose higher and higher, there have more and more  $\text{Cu}_2\text{O}$  crystals' nano-platelates were formed, many nano-platelates assemble together to form just like a structure. Fig. 2 can give some evidences in focus. The contrastive FESEM of sample 6 is shown in Fig. 2f. There have many  $\text{Cu}_2\text{O}$  nanocrystals and not get together to form platelates.

The crystal orientation and crystallinity of  $\text{Cu}_2\text{O}$  crystals nano-platelate are further studied with SAED (Fig. 3a-b). In this measurement, SAED image was recorded by aligning the electron beam parallel to the  $[1\bar{1}1]$  zone axis. From Fig. 2f, there are three sets of distinct lattice spacing of *ca.* 0.30, 0.45 and 0.26 nm, which correspond to the (001), (010) and (011) planes of  $\text{Cu}_2\text{O}$ , respectively, indicating the high crystallinity of the single nano-platelate.

The possible formation mechanism of  $\text{Cu}_2\text{O}$  may be as follows:

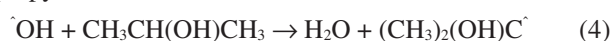
Radiolysis of water:



Reduction of  $\text{Cu}^{2+}$  to  $\text{Cu}^+$ :



Some oxidative radicals such as  $\cdot\text{OH}$  were scavenged by isopropyl alcohol.



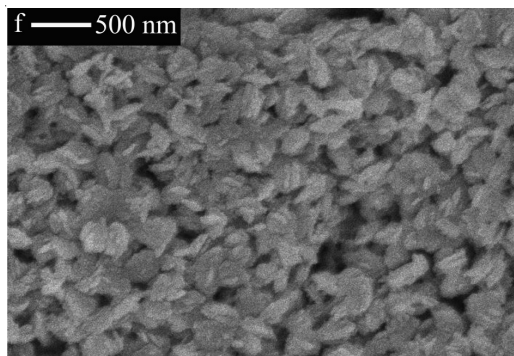
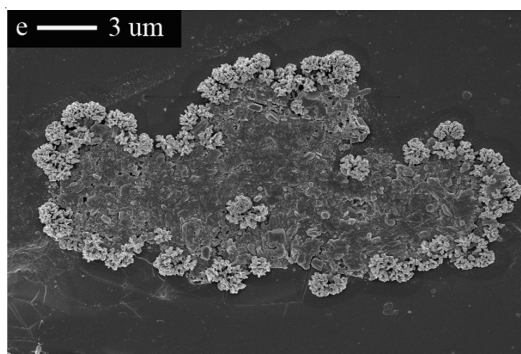
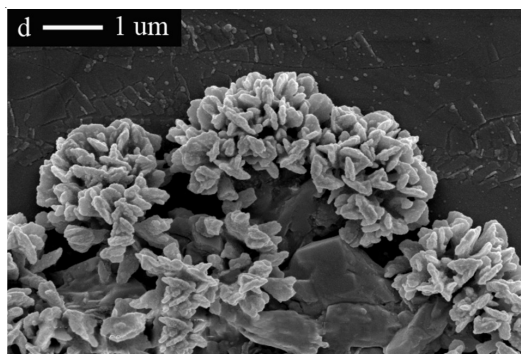
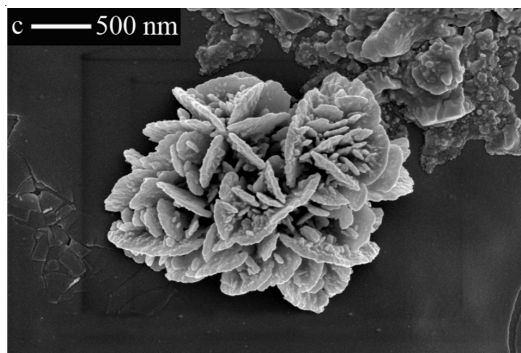
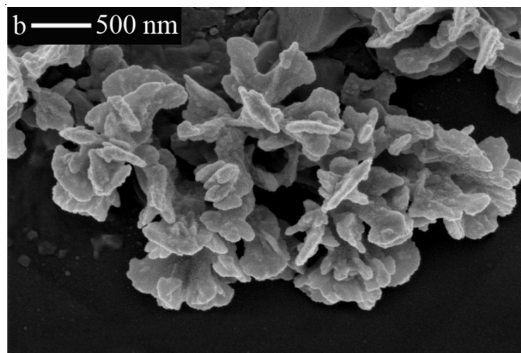
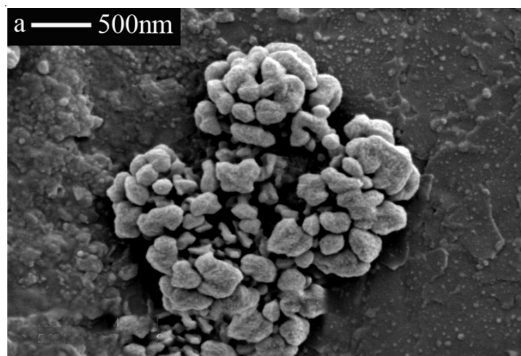


Fig. 2. FESEM of sample (1) a, (2) b, (4) d, (5) e and FESEM of a special area of sample (5) c; FESEM of sample (6) f (without PEG)

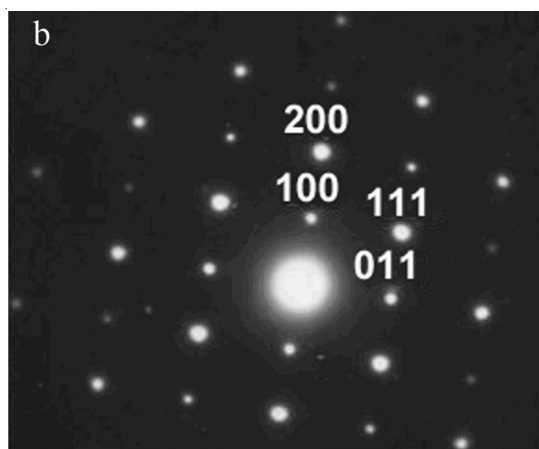
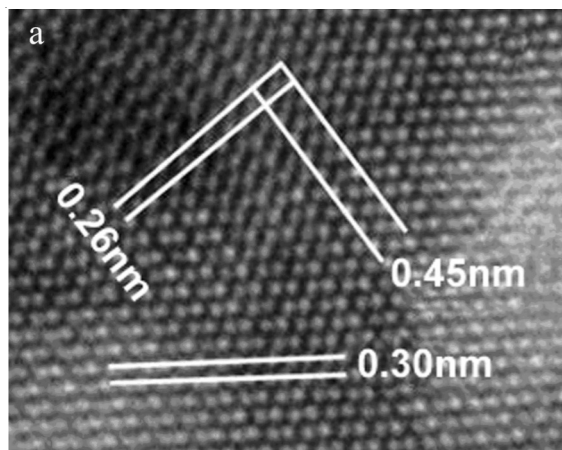


Fig. 3. (a) A lattice-resolved HRTEM image of sample 5 (b) ED pattern taken on the tip of the inset of sample 5

First, the  $\gamma$ -radiolysis of water produce many active intermediates, such as strong reductive hydrated electrons (-2.77 eV) and oxidative radicals  $\cdot\text{OH}$  (eqn. 1). Isopropyl alcohol is introduced to scavenge  $\cdot\text{OH}$  and the obtained  $\text{CH}_3\text{COHCH}_3$  (eqn. 4) radicals also possess reducibility (-1.1 V), which keeps the system under a reductive condition<sup>20</sup> together with  $e_{\text{aq}}^-$ . Secondly, after  $\text{Cu}^{2+}$  has been coordinated with EDTA to form  $[\text{Cu}(\text{II})(\text{EDTA})]^{2-}$ , it would be reduced into  $\text{Cu}^+$  by  $e_{\text{aq}}^-$  subsequently. At last,  $\text{OH}^-$  quickly combines with  $\text{Cu}^+$  to form  $\text{CuOH}$ , which finally decomposes into  $\text{Cu}_2\text{O}$  (reaction 2). On the other hand, the  $\text{CuO}$  particles from the decomposition of  $\text{Cu}(\text{OH})_2$  are then reduced to  $\text{Cu}_2\text{O}$  by  $e_{\text{aq}}^-$ .

At the same, the non-ionized surfactant PEG-400 might be playing an important role during the fabrication of the  $\text{Cu}_2\text{O}$  nano-crystals. As illustrated by Xia and Wang *et al.*<sup>21,22</sup>, the shape of an fcc nano-crystal was mainly determined by the ratio between the growth rates along 100 and 111 directions and the morphologies can be kinetically controlled by adding chemical capping reagents to the synthetic systems. The non-ionized surfactant PEG forms aggregate structure due to the assembly in water<sup>23</sup>. Then a lot of 1D liquid reaction fields could be formed when PEG and a small quantity of water are mixed together. These reaction fields are dispersed in different directions. When a high electric field is provided these reaction fields may be aligned. However, PEG assembly structures in water are flexible and aggregate. Furthermore, the strong affinity of the PEG oxygen atoms for  $\text{Cu}^+$  results in the  $\text{Cu}^+$  adhere to PEG aggregates. Therefore, it is reasonable that the platelated structure  $\text{Cu}_2\text{O}$  was obtained under our experiment condition. Although the exact mechanism for the formation of the platelated structure  $\text{Cu}_2\text{O}$  is still not fully understood, PEG plays important roles in the formation of well-defined  $\text{Cu}_2\text{O}$  nanocrystals with advanced structure.

Fig. 4a. illustrates the UV-VIS absorption spectrum of the  $\text{Cu}_2\text{O}$  platelates dispersed in distilled water. It should be noted that using the data in Fig. 4a showing a considerable blue shifts phenomena of the absorption edge in the transmission spectra of  $\text{Cu}_2\text{O}$  as the amount of platelates are increased. The center absorption peaks position of samples between 290-390 nm (sample 1 to sample 5)<sup>8</sup>. The band gaps of  $\text{Cu}_2\text{O}$

platelates is calculated according to the formula as below:  $(\alpha E_p)^2 = K(E_p - E_g)$  ( $\alpha$  is absorption coefficient,  $K$  is constant,  $E_p$  is photo energy,  $E_g$  is band gaps)<sup>24</sup>. The band gaps of  $\text{Cu}_2\text{O}$  platelates is about 2.25 eV according to the curve  $(\alpha E_p)^2 - E_p$  (Fig. 4b) and bigger than bulk  $\text{Cu}_2\text{O}$  nanomaterials (2.17 eV).

## Conclusion

In summary, a facile method has been developed to prepare micrometer-sized  $\text{Cu}_2\text{O}$  crystals with platelate structure. The preparation of such  $\text{Cu}_2\text{O}$  crystals is carried out under ambient conditions and in  $\gamma$ -irradiation field using PEG as the non-ionized surfactant. The reaction process and shape evolution was investigated by the assistance of XRD and FESEM analyses. The chemical processes can be divided into the following steps: the  $\text{Cu}^{2+}$  ions are converted to  $\text{CuO}$  and  $\text{Cu}_2\text{O}$  in the earlier stage of the reaction, then  $\text{CuO}$  and  $\text{Cu}^{2+}$  ions are consecutively reduced to  $\text{Cu}_2\text{O}$  under our experimental conditions. At the same PEG plays an important role during the formation dendritic  $\text{Cu}_2\text{O}$  with platelate structure and the existence of EDTA ions affects the ratio of the growth rate along the  $\langle 111 \rangle$  versus the  $\langle 100 \rangle$  direction. The UV-VIS absorption peak of  $\text{Cu}_2\text{O}$  platelates appears at about 370 nm and with the corresponding band gap of 2.25 eV, reveals the quantum size effect of  $\text{Cu}_2\text{O}$  platelates.

## ACKNOWLEDGEMENTS

The authors greatly appreciated the help from Central Laboratory of Analysis & Structure Research in University of Science and Technology of China (USTC). This study is financially supported by the National Science Foundation for Post-doctoral Scientists of China (no. 20100471000).

## REFERENCES

1. X. Duan and Y. Cui, *Nature*, **409**, 66 (2001).
2. R.S. Yang, J.R. Morber, L.J. Chou and Z.L. Wang, *Nano Lett.*, **7**, 269 (2007).
3. D. Minamda, S. Okada, M. Hashizume, J.I. Kikuchi, T. Imori and N. Hosoito, *J. Sol-Gel Sci. Technol.*, **48**, 95 (2008).
4. B. Nikoobakht, *Chem. Mater.*, **19**, 5279 (2007).
5. Y. Xiong and Y. Xia, *Adv. Mater.*, **19**, 3385 (2007).
6. T. Borowski, *Asian J. Chem.*, **21**, 4932 (2009).
7. R.N. Briskman, *Sol. Energy Mater. Sol. Cells*, **27**, 361 (1992).
8. M. Yin, C.K. Wu, Y.B. Lou, C. Burda, J.T. Koberstein, Y.M. Zhu and S. O'Brien, *J. Am. Chem. Soc.*, **127**, 9506 (2005).
9. L.L. Ma, Y.L. Lin, J.L. Li, M.Q. Qiu and Y. Yu, *J. Phys. Chem.*, **112**, 18916 (2008).
10. J.N. Gao, Q.S. Li, L.S. Li, Q.H. Gong and L.M. Qi, *Chem. Mater.*, **20**, 6263 (2008).
11. E. Comini, C. Baratto, G. Faglia and A. Vomiero, *Prog. Mater. Sci.*, **54**, 1 (2009).
12. S. Kose, F. Atay, V. Bilgin and I. Akyuz, *Mater. Chem. Phys.*, **111**, 351 (2008).
13. C.Q. Chen, Y.H. Zheng, Y.Y. Zhan, X.Y. Lin, Q. Zheng and K.M. Wei, *Cryst. Growth. Des.*, **8**, 3549 (2008).
14. R. Garuthara and W. Siripala, *J. Lumin.*, **121**, 173 (2006).
15. F.L. Du, J.G. Liu and Z.Y. Guo, *Mater. Res. Bull.*, **44**, 25 (2009).
16. J.N. Nian, C.C. Hu and H.S. Teng, *Int. J. Hydro. Energy*, **33**, 2897 (2008).
17. J.M. Hong, J. Li and Y.H. Ni, *J. Alloys Compd.*, **481**, 610 (2009).
18. C.H. Kuo, C.H. Chen and M.H. Huang, *Adv. Funct. Mater.*, **17**, 3773 (2007).
19. W. Yu, H.Q. Xie, L.F. Chen and Y. Li, *Asian J. Chem.*, **21**, 6927 (2009).
20. G.V. Buxton, *Radiation Chemistry Principles and Applications*, VCH Publishers, New York, pp. 4/321-4/342 (1987).
21. Y.G. Sun and Y.N. Xia, *Science*, **298**, 2176 (2002).
22. Z.L. Wang, *J. Phys. Chem. B*, **104**, 1153 (2000).
23. X.L. Gou, F.Y. Cheng, Y.H. Shi, L. Zhang, S.J. Peng, J. Chen and P.W. Shen, *J. Am. Chem. Soc.*, **128**, 7222 (2006).
24. M. Yang and J.J. Zhu, *J. Cryst. Growth*, **256**, 134 (2003).

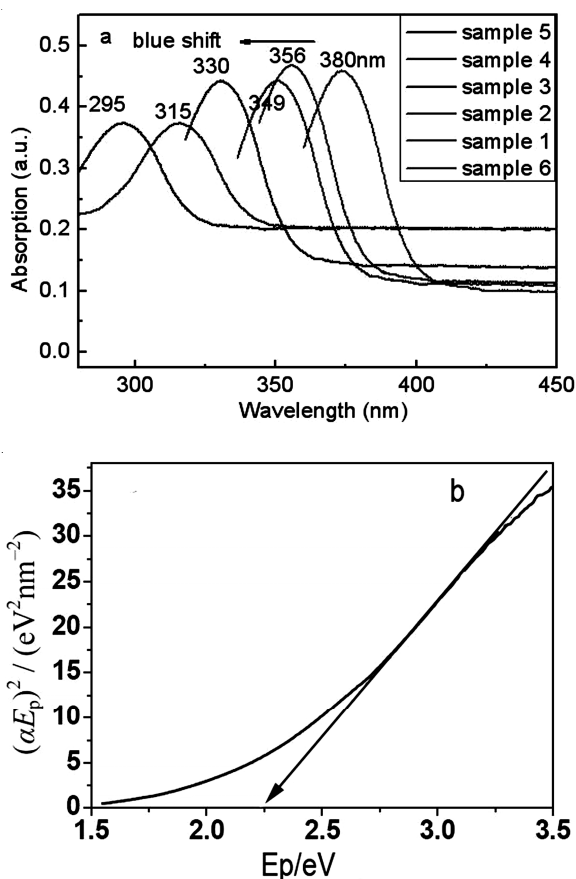


Fig. 4. (a) UV-VIS absorption spectra and (b)  $(\alpha E_p)^2 - E_p$  curve of  $\text{Cu}_2\text{O}$  platelates